CHARACTERIZATION OF THE MORPHOMETRY OF IMPACT CRATERS HOSTING POLAR DEPOSITS IN MERCURY'S NORTH POLAR REGION. Matthieu J. Talpe[1], Maria T. Zuber[1], Gregory A. Neumann[1,2], Erwan Mazarico[1], Sean C. Solomon[3], and Faith Vilas[4]. [1]Department of Earth, Atmospheric, and Planetary Sciences, Massachusetts Institute of Technology, Cambridge, MA 02139 (mtalpe@mit.edu); [2]Planetary Geodynamics Laboratory, Goddard Space Flight Center, Greenbelt, MD 20771; [3]Department of Terrestrial Magnetism, Carnegie Institution of Washington, Washington, DC 20015; [4]Planetary Science Institute, Tucson, AZ 85719.

Introduction: Earth-based radar images dating back two decades show that the floors of some polar craters on Mercury host radar-bright deposits that have been proposed to consist of frozen volatiles (Fig. 1) [1]. Several hypotheses have been put forth to explain their source, including volcanic outgassing, chemical sputtering, and deposition of exogenous water ice [2, 3, 4]. Calculations show that volatiles are thermally stable in permanently shadowed areas [5]. An earlier study of the depths of north polar craters determined with photoclinometric techniques applied to Mariner 10 images yielded the conclusion that the mean ratio of crater depth d to rim-crest diameter D for craters hosting polar deposits is two-thirds that of the mean ratio for a comparable population of neighboring craters lacking such deposits [6]. This result could be explained by (though doesn't require) the presence of a thick layer of volatiles within the polar deposit-hosting craters.

Here we use altimetric profiles and topographic maps obtained by the Mercury Laser Altimeter (MLA) to revisit this analysis. MLA is an instrument on the MErcury Surface, Space ENvironment, GEochemistry, and Ranging (MESSENGER) spacecraft, which has been orbiting Mercury since March 2011. MLA transmits a 1064-nm laser pulse at 8 Hz during MESSENGER's trajectory over Mercury's surface [7]. The MLA illuminates surface areas averaging between 15 m and 100 m in diameter, spaced ~400 m apart along the spacecraft ground track [8]. The radial precision of individual measurements is <1 m, and the current accuracy with respect to Mercury's center of mass is better than 20 m. As of mid-December 2011, MLA coverage had reached to 15°S and has yielded a comprehensive map of the topography of Mercury's northern hemisphere [8]. The MLA data are used here to quantify the shapes of craters in the north polar region and to avoid the shadowing bias of photoclinometric techniques.

Data: We use MLA-derived digital elevation models of the northern hemisphere and 407 MLA altimetry tracks acquired between 29 March 2011 and 6 December 2011. The 3,578,166 altimetry points used are taken exclusively from MLA's channel 0 to minimize instrument error. Mercury Dual Imaging System (MDIS) images are used to aid in crater selection and provide qualitative validation to measurements.

Methodology: Craters are selected from an MLA-derived digital elevation model and are traversed by at least two MLA profiles (see Fig. 1A). At least two MLA profiles are necessary to constrain the location of the rims corresponding to the maxima of the elevation profiles. Crater rim locations are visually inspected to discard rim locations erroneously selected from high surrounding topography not morphologically associated with the crater (see Fig. 2). Crater diameters are computed from a least-squares best-fit circle with respect to the associated rims. Crater depths are computed from the difference between the average rim elevation and the depth of the lowest 10% altimetry points along the most crater-centric MLA profile, which is the most representative profile of crater morphology. The lowest 10% altimetry points are from the crater floor and are validated visually in order to discard unrepresentative depths due to smaller craters superimposed on the floor of the crater studied. Crater wall angles are also measured from the most crater-centric MLA profile for complex craters. The transition diameter D_t between simple and complex craters for Mercury is ~11 km [9].

Results: We selected and measured 274 craters between 6.08 and 207 km in diameter and located between 48 and 87°N. Craters are described by three parameters: location (124 craters in the northern volcanic plains versus 150 in heavily cratered terrain), morphology (28 simple versus 246 complex), and radar brightness (35 with radar-bright deposits versus 239 without such deposits) (see Fig. 1B).

The physiographic difference between the heavily cratered terrain and the northern volcanic plains induces a geographic bias in the type of crater selected. The northern smooth plains, a large expanse of material emplaced by flood volcanism [10], render small craters more readily visible to MLA observations. On the other hand, the sample of complex craters represents a larger fraction of the total crater population in heavily cratered terrain. Consequently, 22 of the 28 simple craters are found in the northern plains. Additionally, 30 of the 35 craters hosting radar-bright polar deposits are located in the northern plains. This difference presumably reflects the latitudinal distribution of the two terrain types.

MESSENGER's eccentric orbit further influences crater selection. Simple craters are measured only at higher latitudes where there is denser MLA coverage. Simple craters are seen at lower latitudes, but the sepa-

ration between MLA tracks increases with latitude and reduces the likelihood of two tracks traversing a given small crater.

Discussion: The *d*/*D* ratios of craters hosting polar deposits are larger than craters lacking such deposits at the 95% significance level, which eliminates the need to account for large volumes of volatiles [6] but requires an explanation for the anomalously large *d*/*D* ratios. Furthermore, crater wall angles aren't significantly steeper for craters hosting polar deposits than for other craters. Thus, increased radiation effects from steeper walls need not be invoked in modeling the thermal properties of the radar-bright deposits inside craters [6].

There are also morphologic distinctions between craters in the northern plains and those in adjacent heavily cratered terrain. Complex craters with diameters less than 50 km (a criterion necessary to compare samples of similar sizes because of selection biases discussed above) in the northern plains are deeper than in heavily cratered terrain. Moreover, steeper walls for craters with diameters greater than 50 km are observed in the northern plains. These morphometric differences are consistent with more advanced degradation states for craters in heavily cratered terrain. In a similar manner, craters in the lunar highlands tend to possess more subdued morphologies than craters in the maria [12]. Such subdued morphologies, the result of greater surface ages, translates to lower *d*/*D* ratios and greater dispersion in the depth-to-diameter plot (see Fig. 3).

The *d*/*D* ratios of craters hosting polar deposits on Mercury are independent of location and are more consistent with the *d*/*D* ratios of the craters in the northern plains, even for craters with polar deposits located in heavily cratered terrain. Thus, it appears that the main difference between craters that do and do not host radar-bright polar deposits is their average degradation state.

Further MLA data will allow the study of craters currently traversed by only one altimetry track and the analysis of surface roughness in crater interiors and their surroundings [13]. Such additional data should also provide information on the poorly covered regions north of 84.5°N where large concentrations of radar-bright deposits are found.

References: [1] Harmon J. K. et al. (2011) *Icarus 211*, 37-50. [2] Potter A. E. (1995) *Geophys. Res. Lett. 22*, 3289-3292. [3] Barlow N. G. et al. (1999) *Icarus 141*, 194-204. [4] Moses J. I. et al. (1999) *Icarus 137*, 197-221. [5] Paige D. A. et al. (1992) *Science 258*, 643-646. [6] Vilas F. et al. (2005) *Planet. Space Sci. 53*, 1496-1500. [7] Cavanaugh J. F. et al. (2007) *Space Sci. Rev. 131*, 451-479. [8] Zuber M. T. et al. (2012) *Science,* submitted. [9] Pike R. J. (1988) in *Mercury*, pp. 165-273. [10] Head J. W. et al. (2011) *Science 333,* 1853-1856. [11] Squyres S. W. and Carr M. H. (1986) *Science 231*, 249-252. [12] Talpe M. T. et al. (2011) *LPS 42*, 2549. [13] Kreslavsky M. A. and Head J. W. (2000) *JGR 105*, 26695-26711.

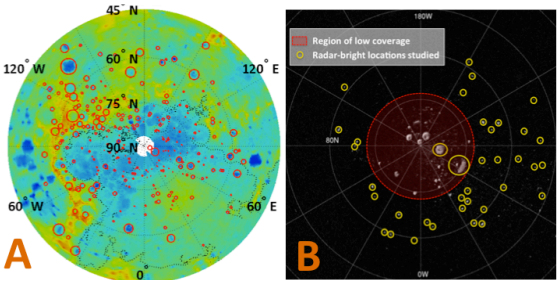

Figure 1. Stereographic views of Mercury's north polar region. (A) Topography. Red circles represent the 274 craters traversed by two or more MLA profiles [8]. The black line delimits the northern volcanic plains. (B) Distribution of craters hosting polar deposits in this study [1]. MLA tracks are sparse poleward of 84°N.

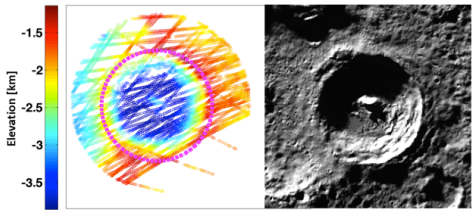

Figure 2. MLA coverage and MDIS image of a complex crater (32.4 km diameter) located at 82.9°N, 208.4°E.

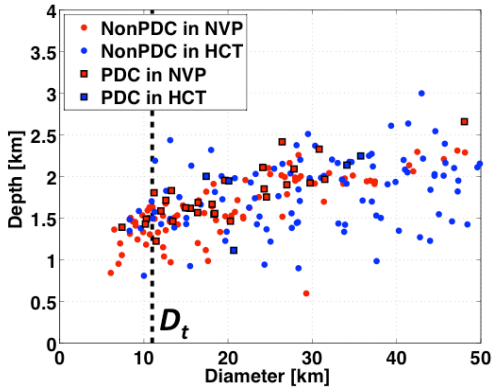

Figure 3. Crater depth versus rim diameter for north polar craters less than 50 km in diameter. Craters hosting polar deposits (PDC) are statistically deeper at the 95% confidence level than craters that lack such deposits (NonPDC), regardless of their geographic location. Craters located in the northern volcanic plains (NVP) are more similar in shape than craters located in heavily cratered terrain (HCT). The regime transition between simple and complex crater morphology is represented by the dashed line at the transition diameter value D_t.